Electronic Supplementary Information

Construction of a dual-functional dumbbell probe-based fluorescent biosensor for cascade amplification detection of miRNAs in lung cancer cells and tissues

Qian Zhang,[‡a] Yun Han, [‡a] Chen-chen Li,[‡b] Xiaoran Zou, [a] Fei Ma, *[,c] Chun-yang Zhang *[,a]

[a] College of Chemistry, Chemical Engineering and Materials Science, Shandong Normal University, Jinan 250014, China.

[b] College of Chemistry and Molecular Engineering, Qingdao University of Science and Technology, Qingdao 266042, China.

[c] School of Chemistry and Chemical Engineering, Southeast University, Nanjing, 211189, China.

[*] Corresponding author. E-mail: fei@seu.edu.cn; cyzhang@sdnu.edu.cn.

[‡] These authors contributed equally.

EXPERIMENTAL SECTION

Chemicals and materials

All oligonucleotides (Table S1) were purchased from TaKaRa Biotechnology Co., Ltd. (Dalian, China). Mir-X miRNA qRT-PCR TB Green® Kit and RNase inhibitor were purchased from TaKaRa Biotechnology Co., Ltd. (Dalian, China). Bst. DNA Polymerase (large fragment), 10× ThermoPol reaction buffer pack (200 mM trizma hydrochloride (Tris-HCl), 100 mM ammonium sulfate ($(NH_4)_2SO_4$), 100 mM potassium chloride (KCl), 20 mM magnesium sulfate ($MgSO_4$), 1% Triton X-100, pH 8.8), EnGen®Lba Cas12a (Cpf1), 10× NEBuffer 2.1 (100 mM Tris-HCl, 500 mM sodium chloride (NaCl), 100 mM magnesium chloride ($MgCl_2$), 1 mg/mL bovine serum albumin (BSA), pH 7.9), dATP, dTTP and dCTP solution were obtained from New England Biolabs (Beverly, MA, USA). Diethylpyrocarbonate (DEPC)-treated water (RNase free) was purchased from Sangon Biological Engineering Technology & Services Co. Ltd. (Shanghai, China) Human non-small-cell lung cancer (NSCLC) cell lines (human lung adenocarcinoma A549 cell line (A549 cells), human non-small cell lung cancer H460 cell line (H460 cells), human airway epithelial H292 cell line (H292 cells), human lung adenocarcinoma H1975 cell line (H1975 cells), and human bronchoalveolar carcinoma H358 cell line (H358 cells)) were obtained from Cell Bank, Shanghai Institutes for Biological Sciences (Shanghai, China). The paraffin-embedding lung tissue samples of NSCLC patients and healthy persons were obtained from the Affiliated Hospital of Guangdong Medical University (Zhanjiang, Guangdong, China), and the experiments were approved by the ethics committee of the Affiliated Hospital of Guangdong Medical University.

Table S1. Sequences of the Oligonucleotides

note	sequence (5'−3')
miR-486-5p	UCC UGU ACU GAG CUG CCC CGA G
11 bp dumbbell probe	ACT AAA TTC AGG GCC TTT TGG CCC TGA ATT TAG TAA TAA GAG ATC CTG CGG GCA GCT CAG TAC AGG ATC TCT TTT TTT T
12 bp dumbbell probe	ACT AAA TTC AGG GCC TTT TGG CCC TGA ATT TAG TAA TAA GAG ATC CTG TGG GCA GCT CAG TAC AGG ATC TCT TTT TTT T
13 bp dumbbell probe	ACT AAA TTC AGG GCC TTT TGG CCC TGA ATT TAG TAA TAA GAG ATC CTG TAG GGC AGC TCA GTA CAG GAT CTC TTT TTT TT
14 bp dumbbell probe	ACT AAA TTC AGG GCC TTT TGG CCC TGA ATT TAG TAA TAA GAG ATC CTG TAC GGG CAG CTC AGT ACA GGA TCT CTT TTT TTT
primer	TTC TCT TAT T
Cy5-labeled primer	Cy5-TTC TCT TAT T
15 nt crRNA	UAA UUU CUA CUA AGU GUA GAU UGA AUU UAG UAA UAA
16 nt crRNA	UAA UUU CUA CUA AGU GUA GAU UGA AUU UAG UAA UAA G
17 nt crRNA	UAA UUU CUA CUA AGU GUA GAU UGA AUU UAG UAA UAA GA
20 nt crRNA	UAA UUU CUA CUA AGU GUA GAU UGA AUU UAG UAA UAA GAG AA
signal probe	Cy5-CGC TTC CCC GAC TTC -BHQ2
miR-486-5p M1	UCC UCU ACU GAG CUG CCC CGA G
miR-486-5p M2	UCC UCU ACU CAG CUG CCC CGA G

miR-486-5p M3	UCC UCU ACU CAG CUC CCC CGA G
miR-4529-3p	AUU GGA CUG CUG AUG GCC CGU
let-7a	UGA GGU AGU AGG UUG UAU AGU U
miR-486-5p-specific primer	TCC TGT ACT GAG CTG CCC CGA G

Detection of target miR-486-5p

The dumbbell probes were obtained by incubating in a buffer (1.5 mM $MgCl_2$, 10 mM Tris-HCl, pH 8.0) at 95 °C for 5 min and then cooling to room temperature. The whole reaction was carried out in a solution (20 μL) containing different-concentration target miR-486-5p, 1× ThermoPol buffer, 1× NEB buffer 2.1, 10 nM dumbbell probes, 100 nM primers, 100 μM dNTPs (dATP, dTTP, dCTP each), 4 U of Bst. DNA polymerase, 80 nM crRNA, 1.75 μM signal probes, 80 nM Cas12a, and 20 U of RNase inhibitor at 37 °C for 2 h.

Gel electrophoresis and fluorescence measurement

The reaction products were analyzed by using 12% nondenaturing PAGE in 1× TBE buffer (9 mM boric acid, 0.2 mM EDTA, 9 mM Tris-HCl, pH 7.9) at 110 V. After electrophoresis, the gel was imaged by a Bio-Rad ChemiDoc™ MP Imaging System (Bio-Rad, Hercules, CA, USA). A FLS-1000 fluorescence spectrometer (Edinburgh Instruments Ltd., Livingston, United Kingdom) was employed to obtain fluorescence emission spectra. Cy5 dye was excited by a 635 nm laser, and the emission spectrum was recorded from 650 to 750 nm.

Single-molecule detection

The 10 μL of reaction products with 10000-fold dilution was placed on a coverslip for single-molecule fluorescence imaging. The interest regions of 500 × 500 pixels were selected for count-

ing Cy5 molecules by using Image J software. For single-molecule photobleaching experiments, the diluted reaction solution was continuously excited by a 640-nm laser and taken images with a 400-ms exposure time.

The qRT-PCR assay

A Mir-X miRNA qRT-PCR TB Green® Kit was used to quantify total RNA. The poly(A)/cDNA synthesis reaction was performed in a solution (20 μL) containing 2× mRQ buffer (10 μL), total RNA/miR-486-5p, and 2.5 μL of mRQ enzyme under the conditions of 37 °C for 60 min and then 85 °C for 5 min. The qRT-PCR was performed in a solution (12.5 μL) containing 2× TB Green advantage premix (6.25 μL), 10 μM miR-486-5p-specific primer (0.25 μL), 50× ROX reference dye (0.25 μL), 10 μM mRQ 3' primer (0.25 μL), and RT product (1 μL) under the conditions of 95 °C for 30 s, 40 cycles of 95 °C for 5 s and 60 °C for 30 s. A Bio-Rad CFX connect real-time system was employed to obtain the real-time fluorescence.

Cell culture and total RNA extraction

A549 cells were cultured with 1% penicillin-streptomycin and 10 % fetal bovine serum (FBS, gibco, USA) in Dulbecco's modified Eagle's medium (DMEM, gibco, USA). H460 cells, H292 cells, H1975 cells and H358 cells were cultured in RPMI-1640 medium (Gibco, USA) supplemented with 10 % FBS and 1% penicillin-streptomycin. All cells were cultured at 37 °C in a humidified atmosphere containing 5% CO_2. The total RNA was extracted from cancer cells or human tissues using the Qiagen miRNeasy RNA isolation kit (Hilden, Germany) according to the manufacturer's protocol, and the concentration of total RNA was quantified by the NanoDrop 2000c Spectrophotometer (Thermo Scientific, Wilmington, Delaware, USA).

SUPPLEMENTARY RESULTS

Calculation of standard free energy change (*ΔG*) and theoretical conversion efficiency (*E*) for initiating PER

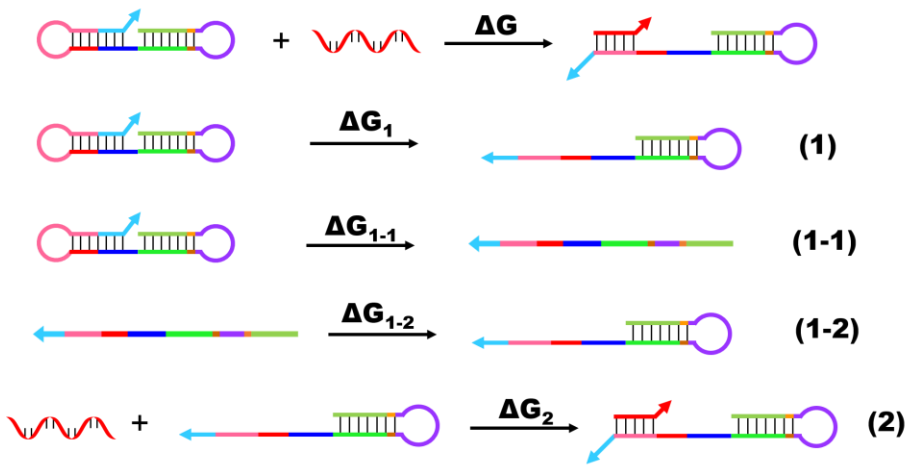

Fig. S1 Scheme of the activation reaction process.

PER is initiated by a toehold-mediated strand displace-ment process. Ideally, the dumbbell probe should possess the characteristics of both stability for resisting nonspecific reaction and flexibility for recognizing target miRNAs and activating subsequent amplification reaction. As shown in Fig. S1, the activation process of PER involves two reactions including the transformation from dumb-bell probe to hairpin probe (step 1) and the hybridization between hairpin probe and miR-486-5p (step 2). To estimate ΔG_1, step 1 reaction can be decomposed into two separate reactions (steps 1-1 and 1-2). The ΔG of each reaction is calculated on the Oligo Analyzer site under the conditions of temperature of 37 °C and salt concentration of 50 mM Na^+ + 12 mM Mg^{2+}. Table S2 lists the ob-tained values. The ΔG of the whole activation process can be determined based on Hess's law:

$$\Delta G = \Delta G_{1-1} + \Delta G_{1-2} + \Delta G_2 \qquad (3)$$

Notably, the ΔG_1 value (10.09 kcal/mol, $\Delta G_1 = \Delta G_{1\text{-}1} + \Delta G_{1\text{-}2}$) of step 1 is positive due to the

self-complementary state of dumbbell probe. When dumbbell probe incubates with miR-486-5p and other miRNAs to perform hybridization reaction, respectively, only the ΔG of the miR-486-5p activation is negative (ΔG = -8.62 kcal/mol), suggesting that only miR-486-5p can initiate the dual signal amplification.

Table S2. The ΔG of each decomposition reaction.

	ΔG (kcal/mol)	$\Delta G_{1\text{-}1}$ (kcal/mol)	$\Delta G_{1\text{-}2}$ (kcal/mol)	ΔG_2 (kcal/mol)
miR-486-5p	-8.62	25.92	-15.83	-18.71
miR-486-5p M1	0.92	25.92	-15.83	-9.17
miR-486-5p M2	8.35	25.92	-15.83	-1.74
miR-486-5p M3	19.58	25.92	-15.83	9.49
miR-4529-3p	13.57	25.92	-15.83	3.48
let-7a	20.79	25.92	-15.83	10.7

We further used the obtained thermodynamic parameters to calculate the theoretical conversion efficiency (*E*) for the PER activation according to the following equations:

$$\Delta G_1 = \Delta G_H - \Delta G_D \quad (4)$$

$$\Delta G_2 = \Delta G_{TD} - \Delta G_T - \Delta G_H \quad (5)$$

where *T*, *H*, *D*, and *TD* are target miR-486-5p, hairpin probe, dumbbell probe, and target miR-486-5p-dumbbell probe hybrids, respectively. We calculated the equilibrium concentrations of all DNA components by introducing two dependent variables (*x* and *y*) and two tunable variables (c_T and c_D) and solving the equations:

$$K_1 = e^{-\frac{\Delta G_1}{RT}} = \frac{[H]}{[D]} = \frac{y}{c_D - x} \quad (6)$$

$$K_2 = e^{-\frac{\Delta G_2}{RT}} = \frac{[TD]}{[T][H]} = \frac{x}{y(c_T - x)} \qquad (7)$$

where c_D = $[D]_0$, c_T = $[T]_0$, x = [TD], and y = [H]. The K value of the whole activation process can be calculated based on Hess's law.

$$K = K_1 K_2 = e^{-\frac{(\Delta G_1 + \Delta G_2)}{RT}} = \frac{x}{(c_D - x)(c_T - x)} \qquad (8)$$

When T = 310.15 K and R = 1.987 × 10^{-3} kcal·K^{-1}·mol^{-1}, we estimated the theoretical conversion efficiency (E) for the PER activation based on equation 9.

$$E = \frac{x}{c_T} \times 100\% \qquad (9)$$

All the theoretical conversion efficiencies are more than 99.99% for the miR-486-5p concentration ranging from 10 fM to 10 nM (Table S3), suggesting that even a few copies of target miR-486-5p can efficiently initiate the PER cascade amplification.

Table S3. Theoretical conversion efficiency (E) for the PER activation induced by different-concentration miR-486-5p.

concentration of miR-486-5p	conversion efficiency (%)
10.0 nM	99.99
1.0 nM	99.99
100.0 pM	99.99
10.0 pM	99.99
1.0 pM	99.99
100.0 fM	99.99
10.0 fM	100.00

Instrumental setup

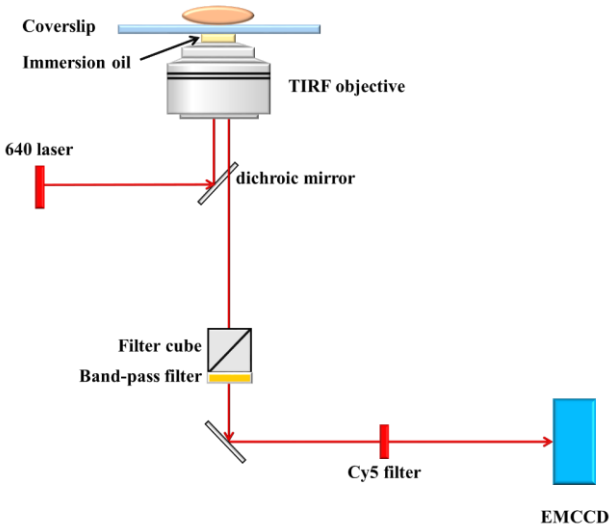

Fig. S2 Schematic diagram of the instrumental setup.

The total internal reflection fluorescence (TIRF) microscope (IX-71, Olympus) is used for single-molecule detection (Fig. S2). A 640 nm laser (50 mW, Coherent) was used to excite Cy5, and the laser beam is reflected by a dichroic mirror and focused on an oil immersion UAPON 100× TIRF objective (1.49 NA, Olympus) to excite the sample pipetted on the coverslip. Photons were then passed through another dichroic mirror and filtered by a Cy5 filter and detected by a chilled charge-coupled-device electron-multiplying (EMCCD) camera (Ixon DU897, Andor).

Optimization of the reaction conditions

To achieve the best assay performance, we optimized several experimental conditions including the left stem length of the dumbbell probe, the length of crRNA, the reaction time, the amount of Bst. DNA polymerase, the concentration of Cas12a-crRNA complex and signal probe. The signal-to-noise ratio (*S/N*) was used to evaluate the assay performance, which represents the ratio of Cy5

signal in the presence of miR-486-5p to that in the absence of miR-486-5p.

The dumbbell probe serves as both a detection probe for target miRNA recognition and a template for PER amplification. We investigated the influence of the stem length of dumbbell probe upon the assay performance. In theory, the longer stem length can better stabilize the stem structure and block nonspecific primer binding to generate a low background, but excessively long stem will hinder the binding of target microRNA with the dumbbell probe to decrease the target signal. We tested five different dumbbell probes with 11, 12, 13, and 14 base pairs (bp) in the left stem region. As shown in Fig. S3A, the S/N value reaches the maximum at a left stem length of 12 bp. Thus, we selected the 12 bp dumbbell probe in the subsequent researches. We further investigated the effect of crRNA length upon the assay performance. A longer crRNA can promote its hybridization with the extended primer to improve Cas12a activity, but excessively long crRNA will increase its hybridization with the unextended primer to decrease the PER amplification efficiency. As shown in Fig. S3B, the S/N value reaches the maximum at a crRNA length of 16 nt. Thus, 16 nt crRNA is used in the subsequent researches. It should be noted that the primer sequence with the capability of both efficient primer extension and product dissociation is directly adopted from the reported literature.[1]

In theory, a longer reaction time can produce a higher signal, but it may inevitably lead to a higher background signal. As shown in Fig. S3C, the *S/N* value gradually enhances with the reaction time, and reaches the maximum at 120 min, followed by decrease beyond 120 min. Thus, 120 min is chosen as the optimized reaction time. Bst. DNA polymerase has strong polymerization activity and strand displacement activity, and the amount of Bst. DNA polymerase may influence the efficiency of PER. In theory, the larger the amount of Bst. DNA polymerase, the higher the

efficiency of PER, but the excess Bst. DNA polymerase may induce nonspecific amplification to produce high background signal. As shown in Fig. S3D, the highest *S/N* value is achieved at 4 U. Therefore, 4 U of Bst. DNA polymerase is used in the subsequent researches.

We further optimized the concentrations of Cas12a-crRNA complex and signal probe. As shown in Fig. S3E, the *S/N* value gradually enhances with the increasing concentration of Cas12a-crRNA complex and reaches a plateau at 80 nM. Thus, 80 nM is selected as the optimal concentration of Cas12a-crRNA complex. As shown in Fig. S3F, the *S/N* value enhances with the increasing concentration of signal probe from 1.25 to 1.75 μM, followed by the decrease beyond 1.75 μM. Thus, 1.75 μM is selected as the optimal concentration of signal probe.

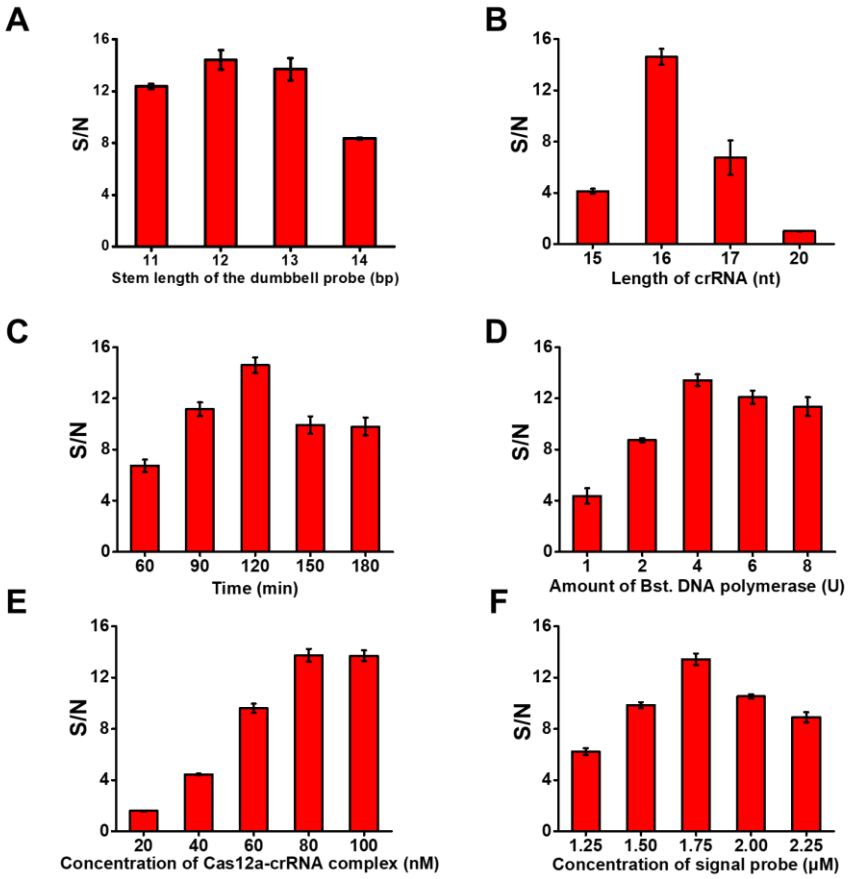

Fig. S3 Optimization of (A) stem length of the dumbbell probe, (B) length of crRNA, (C) reaction time, (D) the Bst. DNA polymerase amount, (E) the Cas12a-crRNA complex concentration, (F) the signal probe concentration. Error bars represent standard deviation of three experiments. The

concentration of miR-486-5p is 10 nM.

The qRT-PCR measurement

The qRT-PCR is used as the reference to demonstrate the reliability and accuracy of this biosensor. The real-time fluorescence curves in response to various-concentration miR-486-5p are shown in Fig. S4. The data were processed by using the comparative C_T (threshold cycle) method. A linear correlation is obtained between the C_T value and the logarithmic of miR-486-5p concentration in the range from 10 fM to100 pM. The regression equation is $C_T = -7.44 - 2.64\log_{10} C_{miR\text{-}486\text{-}5p}$ ($R^2 = 0.996$), where $C_{miR\text{-}486\text{-}5p}$ is the miR-486-5p concentration.

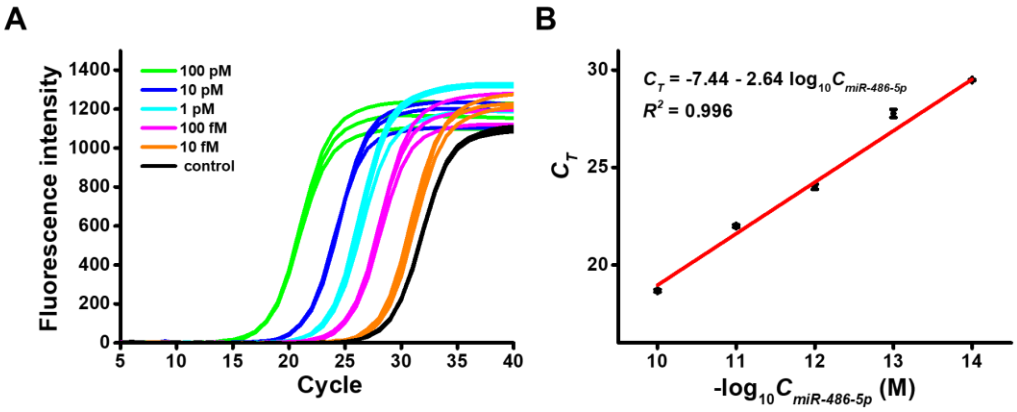

Fig. S4. (A) Real-time fluorescence curves of qRT-PCR generated different concentrations of miR-486-5p ranging from 0 to 100 pM. (B) Linear correlation between the C_T value and the logarithm of miR-486-5p concentration. Error bars are the standard deviation of three experiments.

Table S4. Comparison of the proposed biosensor with the reported methods for miRNA assay.

Method	Required enzymes	Required temperatures	Involved steps	Assay time	Detection limit	references
RCT-CRISPR/Cas12a	(1) SplintR ligase (2) T7 RNA polymerase (3) Exonuclease I (4) Cas12a	(1) 80 °C (2) 37 °C (3) 95 °C	4	~6 h	0.47 amol	[2]
RCA-mediated multiple transcription	(1) T4 polynucleotide kinase (2) T4 DNA ligase (3) phi29 DNA polymerase (4) Klenow Fragment (3′ → 5′ exo-) DNA polymerase (5) T7 RNA polymerase	(1) 37 °C (2) 65 °C (3) 30 °C	3	~6.5 h	67.3 fM	[3]
RCA-CRISPR/Cas12a	(1) T4 DNA ligase (2) phi29 DNA polymerase (3) Cas12a	(1) 95 °C (2) 16 °C (3) 60 °C (4) 37 °C	4	~4 h	34.7 fM	[4]
CRISPR/Cas12a-mediated cascade enzymatic amplification	(1) T4 RNA ligase (2) T7 RNA polymerase (3) Cas12a	(1) 65 °C (2) 25 °C (3) 37 °C	4	~4 h	21.9 fM	[5]
HRCA- and transcription- assisted CRISPR/Cas12a-based strategy	(1) SplintR ligase (2) phi29 DNA polymerase (3) T7 RNA polymerase (4) Cas12a	(1) 85 °C (2) 37 °C (3) 95 °C (4) 30 °C (5) 80 °C (6) 70 °C (7) 65 °C	4	~7 h	1 fM	[6]
HRCA-based QD biosensor	(1) Bst. DNA polymerase	(1) 95 °C (2) 60 °C (3) 80 °C (4) 45 °C	3	~3.5 h	0.72 fM	[7]
PER-CRISPR/Cas12a	(1) Bst. DNA polymerase (2) Cas12a	(1) 37 °C	1	~2 h	0.45 fM (or 9 zmol)	This work

Note: RCT: rolling circle transcription; RCA: rolling circle amplification; HRCA: hyperbranched rolling circle amplification.

Table S5. Recovery study by spiking miR-486-5p into 10% normal human serum.

sample	added (pM)	measured (pM)	recovery (%)	RSD (%)
1	10.0	10.01	100.01	1.50
2	5.00	4.97	99.30	0.93
3	2.00	1.97	98.58	0.30
4	1.00	1.01	100.60	0.56
5	0.20	0.20	99.60	0.30

Table S6. Measurement of miR-486-5p in tissue samples from five healthy persons and five NSCLC patients.

sample	Cy5 counts	miR-486-5p concentration (pM, by proposed method)	median concentration (pM)	C_T value	miR-486-5p concentration (pM, by qRT-PCR)	median concentration (pM)
normal 1	1946.5 ± 0.71	12.95 ± 0.09		20.87 ± 0.05	14.47 ± 0.55	
normal 2	1954 ± 7.07	13.8 ± 0.45		20.81 ± 0.16	14.45 ± 1.63	
normal 3	1894.5 ± 12.02	9.24± 0.75	9.63	22.35 ± 1.52	9.59 ± 0.34	10.30
normal 4	1789 ± 16.97	4.78 ± 0.44		22.35 ± 0.10	4.26 ± 0.37	
normal 5	1858.5 ± 3.53	7.37 ± 0.18		21.41 ± 0.13	8.74 ± 0.08	
patient 1	1755 ± 11.31	3.81 ± 0.26		22.44 ± 0.10	3.92 ± 0.32	
patient 2	1631 ± 30.8	1.74 ± 0.34		23.50 ± 0.52	1.72 ± 0.64	
patient 3	1607.3 ± 38.17	1.51 ± 0.34	1.92	23.96 ± 0.18	1.17 ± 0.16	1.96
patient 4	1644 ± 15.56	1.87 ± 0.18		23.28 ± 0.23	1.97 ± 0.36	
patient 5	1481.5 ± 30.40	0.66 ± 0.11		24.07 ± 0.13	1.01 ± 0.11	

REFERENCES

1. J. Y. Kishi, T. E. Schaus, N. Gopalkrishnan, F. Xuan and P. Yin, *Nature Chemistry*, 2018, **10**, 155-164.
2. G. Wang, W. Tian, X. Liu, W. Ren and C. Liu, *Anal. Chem.*, 2020, **92**, 6702-6708.
3. X. Tang, R. Deng, Y. Sun, X. Ren, M. Zhou and J. Li, *Anal. Chem.*, 2018, **90**, 10001-10008.
4. G. Zhang, L. Zhang, J. Tong, X. Zhao and J. Ren, *Microchem. J.*, 2020, **158**, 105239.
5. H. H. Sun, F. He, T. Wang, B. C. Yin and B. C. Ye, *Analyst*, 2020, **145**, 5547-5552.
6. W. Tian, X. Liu, G. Wang and C. Liu, *Chem. Commun.*, 2020, **56**, 13445-13448.
7. J. Hu, M. H. Liu and C. Y. Zhang, *Chem. Sci.*, 2018, **9**, 4258-4267.